

Effects of Oxygen Content on the Melting Characteristics and Brazing Mechanical Properties of Silver-based Powder Brazing Filler Metals

Long Fei¹, Zhang Guanxing², He Peng^{1,2}, Geng Huiyuan¹, Ding Tianran², Ma Jia²

¹ State Key Laboratory of Advanced Welding and Joining, Harbin Institute of Technology, Harbin 150006, China; ² State Key Laboratory of Advanced Brazing Filler Metals & Technology, Zhengzhou Research Institute of Mechanical Engineering Co., Ltd, Zhengzhou 450001, China

Abstract: Density functional theory (DFT) calculations and various analytical methods were employed to study the effects of increased oxygen content on the melting characteristics and brazed joint mechanical properties. The results reveal that the apparent activation energy of the filler metal increases with increasing the oxygen content, resulting in an increase in the melting time. The tensile strength of the brazed joints decreases nonlinearly with increasing the oxygen content in the filler metal. To ensure the good performance of brazing filler metals, oxygen content of the filler metals should be controlled less than 200 $\mu\text{g}\cdot\text{g}^{-1}$. According to the fatigue testing results, the brazing defects induced by oxygen serve as a source of fracture cracks. This study provides a detailed mechanism of the effects of oxygen on the brazing process of the silver-based powder filler metals.

Key words: oxygen content; melting characteristics; mechanical properties

The brazing process, as an “universal glue”, is widely used in aerospace, electrical appliances, automobile industries, electronic information, and refrigeration applications. Due to its low melting temperature, good liquidity, high joint strength, good-looking brazing beam, and other positive features, silver-based powder brazing filler metals are often applied in the brazing process^[1-4]. Present studies on the silver-based brazing filler metals mainly are focused on the effects of alloying elements, such as lead, bismuth, aluminum, iron, calcium, and sulfur^[5]. In addition, silver-based powder brazing filler metals easily suffer the increase in oxygen level because of the higher surface area ratio. Such increased oxygen level usually degrades the performance of the brazed joint. However, few systematic studies have been conducted on the effect of oxygen content on the performance of silver-based powder brazing filler metals. The detailed mechanism of the oxygen absorption and its effects on the brazing performance are still unclear. Therefore, it is of great theoretical and practical significance to study these effects, with the goal of

improving brazing quality^[2,6].

In this paper, the commonly-used silver-based powder filler metal FAg737 (specific ingredients: Ag29Cu24.5Zn23.5Cd19Sn4) was used as an exemplary filler metal in this study. The effects of total oxygen content on the melting properties and brazing performance were systematically studied, which will provide important technical information for brazing filler metal producers and users^[7].

1 Experiment

To accelerate the oxygen absorption, the as-cast FAg737 powders were annealed (in air) at 300 °C for different time. The gas content of the powder brazing filler metals was measured using a TCH-600 gas spectrometer (LECO Co., St. Joseph, MI, USA) with pulsed current sample heating. The dynamic and carrier gas pressures were 0.28 and 0.14 MPa, respectively. The lowest and highest analysis powers were 900 and 3000 W, respectively. The exhaust power was set to 45 000 W, with a total oxygen analysis time of 80 s. The

Received date: February 28, 2019

Foundation item: Science and Technology Innovation Talents Program of Henan Province (174200510010)

Corresponding author: He Peng, Professor, State Key Laboratory of Advanced Welding and Joining, Harbin Institute of Technology, Harbin 150006, P. R. China, Tel: 0086-451-86402787, E-mail: hithepeng@hit.edu.cn

Copyright © 2020, Northwest Institute for Nonferrous Metal Research. Published by Science Press. All rights reserved.

sample powders were placed into a high purity graphite crucible by means of a feeding device. High purity helium gas (purified by anhydrous magnesium perchlorate and alkaline asbestos treatment) carried the gas released by the powders. Released gas first arrived at the CO and CO₂ detector cells and then passed over heated copper oxide to convert CO to CO₂. Finally, the gas passed through an infrared detector with a low CO₂ content. The oxygen content was measured via two CO₂ infrared detectors and one CO infrared detector.

The formation enthalpies of several possible oxides were calculated by the density functional theory (DFT) method implanted in the full potential SPR-KKR software. The calculations were performed in the fully relativistic mode by solving the Dirac equation for core and valence states. Moruzzi, Janak, and Williams (mjlw) method was used for the parameterization of the exchange energy. The k-integration mesh was set to a size of (7×7×7) during the self-consistent cycles (213 k-points in the irreducible wedge of the Brillouin zone). The crystal potential was converged self-consistently. The self-consistency cycles were repeated until input-output differences of the potentials and charges inside the muffin-tin spheres were of the order of 1.36×10⁻⁴ MeV and 10⁻³ e, respectively.

The solidus temperature of the brazing alloy was measured using a STA449F3 thermal analyzer (Netzsch Instruments North America, LLC, Boston, MA, USA) with a heating rate of 10 K/min. The alloy microstructure was analyzed using a ZEISS metallographic microscope (Carl Zeiss Microscopy GmbH, Jena, Germany)^[8-10].

The joint tensile test was performed according to the Chinese National Standard GB/T 11363-2008. Fig.1 shows the shape and size of the joint. Defect-free tensile specimens with a clean surface were obtained by cleaning, machining, and polishing the joints after brazing. Tensile tests were carried out using a MTS E45.105 mechanical testing machine (MTS Systems Co., Eden Prairie, MN, USA) with a beam moving speed of 0.05 mm/s.

2 Results and Discussion

2.1 Effects of oxygen content on melting characteristics of the silver-based brazing filler metal

Table 1 lists the measured oxygen content of samples with different annealing time. The oxygen content increases gradually with increasing the annealing time. Fig.2 shows the solidus temperatures of brazing filler metals with different oxygen contents. It is clear that the solidus temperature increases linearly with increasing the oxygen content, indicating a higher brazing temperature.

Taking No.1 (as-cast, with oxygen content of 26 μg·g⁻¹) and No.6 (annealed, with oxygen content of 2300 μg·g⁻¹) samples as examples, the phase transition dynamics and thermal kinetic analyses were performed. Fig.3 shows the differential scanning calorimetry (DSC) curves and the reaction fraction α of the two samples. Here the reaction fraction α is equal to the ratio of the reaction heat H_t of a sample at time t to the total heat released H_0 of the sample after the reaction completion, i.e. $\alpha=H_t/H_0$. Notably, H_0 corresponds to the total area under the DSC curve. Using the Proteus analysis software, the total areas under the endothermic peak curve in Fig.3a and 3b are calculated to be 40.02 and 20.08 J/g, respectively.

According to the differential non-isothermal method of thermogravimetric analysis, the kinetic equation (model) is generally expressed by the following equation^[11]:

$$\frac{d\alpha}{dT} = \frac{A}{\beta} e^{-\frac{E}{RT}} f(\alpha) \quad (1)$$

where $f(\alpha)$ is the differential mechanism function of the reaction process, which is defined as:

$$f(\alpha) = (1-\alpha)^n \quad (2)$$

Therefore, the differential equation of the reaction process is expressed as:

$$\frac{d\alpha}{dT} = \frac{A}{\beta} e^{-\frac{E}{RT}} (1-\alpha)^n \quad (3)$$

where T is the reaction temperature, in K; A is the pre-exponential factor; β is the heating rate, in K/min; E is the activation energy, in J/mol; R is the molar gas constant, 8.3145 J·mol⁻¹·K⁻¹; and n is the function's power.

Following Eq.(3), one obtains:

$$\frac{\Delta \lg\left(\frac{d\alpha}{dT}\right)}{\Delta \lg(1-\alpha)} = -\frac{E}{2.303R} \cdot \frac{\Delta\left(\frac{1}{T}\right)}{\Delta \lg(1-\alpha)} + n \quad (4)$$

Eq.(4) is also called as the Freeman-Carroll method. Therefore, the activation energy E can be obtained by the linear fitting of Eq.(4) to obtain the values of $\Delta\left(\frac{1}{T}\right)/\Delta \lg(1-\alpha)$ and $\Delta \lg\left(\frac{d\alpha}{dT}\right)/\Delta \lg(1-\alpha)$, as shown in Fig.4a and 4b. According

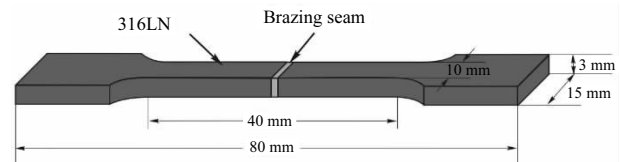


Fig.1 Shape and size of tensile specimens

Table 1 Oxygen content of samples with different annealing time

Samples No.	1	2	3	4	5	6	7	8	9
Annealing time/min	-	-	5	10	30	60	90	120	180
Oxygen content/μg·g ⁻¹	26	110	203	320	1600	2300	3836	4817	6047

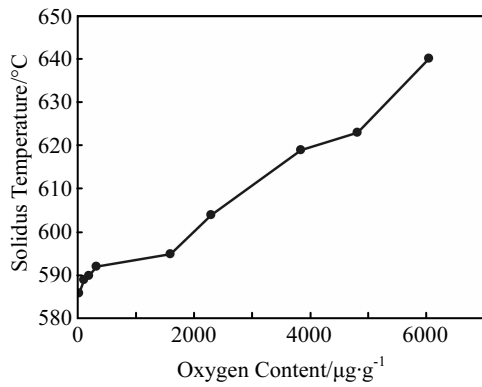


Fig.2 Solidus temperature of samples with different oxygen contents

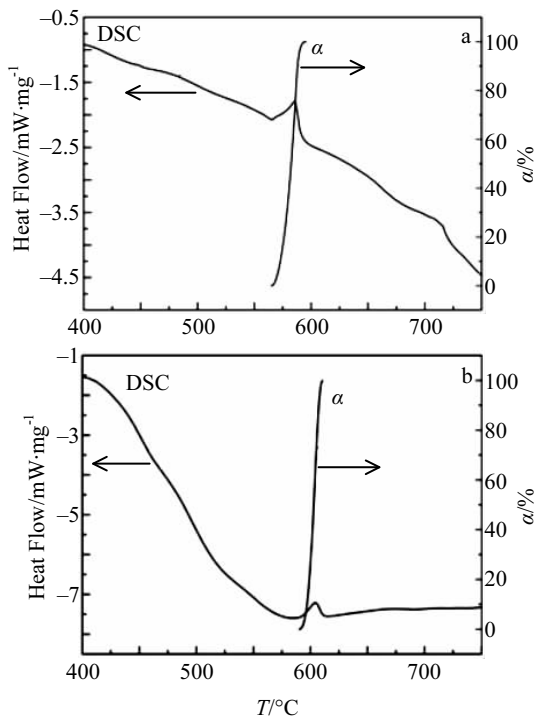


Fig.3 DSC and reaction fraction α curves for the samples with different oxygen contents: (a) $26 \mu\text{g}\cdot\text{g}^{-1}$ and (b) $2300 \mu\text{g}\cdot\text{g}^{-1}$

to the fitting results, the activation energy of the phase transition of the two kinds of powder brazing filler metals is 46.554 and 77.564 kJ/mol, respectively.

From the above analysis, the increase in oxygen content remarkably improves the solidus temperature of the brazing filler metal and the apparent activation energy required for transition from solid to liquid state. As a result, the melting time of the powder brazing filler metals under the same conditions is extended.

2.2 Effect of oxygen content on mechanical properties of brazed joints

Brazing filler metals with different oxygen contents were

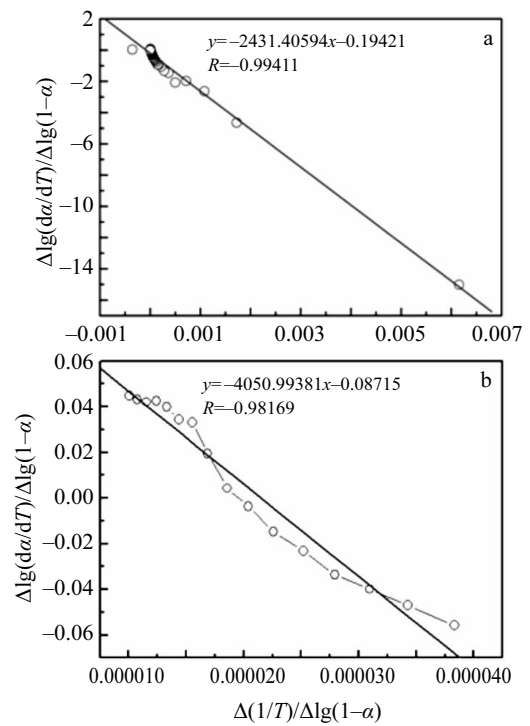


Fig.4 Numerical fitting results of sample 1 (a) and sample 6 (b)

used to braze 316LN stainless steel butt joints, which were then subjected to tensile-strength test (Fig.5)^[12-14]. It is found that the tensile strength of the brazing joint decreases nonlinearly with increasing the oxygen content in the filler metal. When the oxygen content is less than $203 \mu\text{g}\cdot\text{g}^{-1}$, the tensile strength is larger than 350 MPa. When the oxygen content increases from $203 \mu\text{g}\cdot\text{g}^{-1}$ to $320 \mu\text{g}\cdot\text{g}^{-1}$, the tensile strength drops rapidly from 371 MPa to 298 MPa. Thus, in order to ensure the performance of these filler metals, filler metal oxygen content should be controlled below $200 \mu\text{g}\cdot\text{g}^{-1}$.

To further analyze the effects of oxygen content on the mechanical properties of the brazed joints, the microstructures

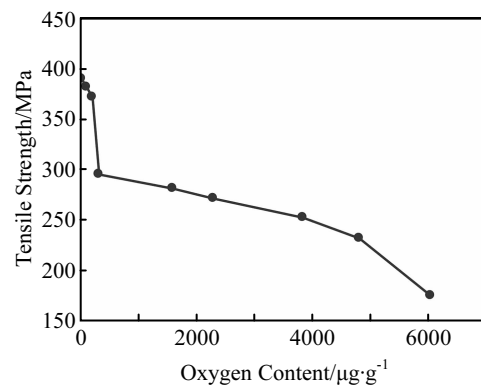


Fig.5 Tensile strength of the brazed joints with different oxygen contents

of three groups of samples (with oxygen content of 26, 320, and $1600 \mu\text{g}\cdot\text{g}^{-1}$) were observed, as shown in Fig.6.

Observation of the samples' microstructure clearly shows that the oxide inclusions in the joints increase with increasing the oxygen content. This explains the lower tensile strength for the brazed joints with higher oxygen content. Fig.7 shows the calculated formation enthalpy of various possible oxides in the FAg737 filler metal. It is clear that the most stable oxide is SnO_2 , and the second one is ZnO in the studied case. Therefore, it can be highly speculated that the oxides in the brazed joint are Sn or Zn based oxides.

The examination of five kinds of broken joints with different oxygen contents shows that the fracture morphology of sample 2 exhibits a reticular distribution and dimples are evenly distributed, exhibiting more obvious toughness-fracture characteristics (Fig.8a). Compared with sample 2, the shape of dimples in sample 4 is different. The reason is that the joint's toughness is altered due to the increase in oxygen content. Also, the number of the micropore nucleus in sample 4 increases. To reduce the surface energy, these pores tend to connect to each other, finally resulting in the joint fracture. In

the samples 5, 6, and 8, the dimples become smaller and some obvious cracks and other brazing defects appear in these samples, indicating the reduced mechanical properties of the brazed joints.

A fatigue test was performed on the 5# brazed joint with an oxygen content of $1600 \mu\text{g}\cdot\text{g}^{-1}$. Before the fatigue test, the filler metal surface is smooth without any visible cracks. But there is an insignificant brazing defect at the upper left corner of the specimen (Fig.9a). After 100 h of fatigue testing, the joint shows a certain degree of plastic deformation (Fig.9b). In addition, there are some deformation bands on the surface. A significant strain concentration occurs at the interface of the upper right corner of the filler metal joint and microcracks appear along the interface. The crack at the brazing defect in Fig.9 is more apparent, indicating that the brazing defect in the fatigue process is the source of cracking.

The crack initiation behavior at the interface and defect was further examined by separately tracking the phenomena at higher magnification^[15]. Before fatigue testing, the interface is well combined, without defects and cracks (Fig.10a). The interface morphology after 100 h of thermal cycling shows

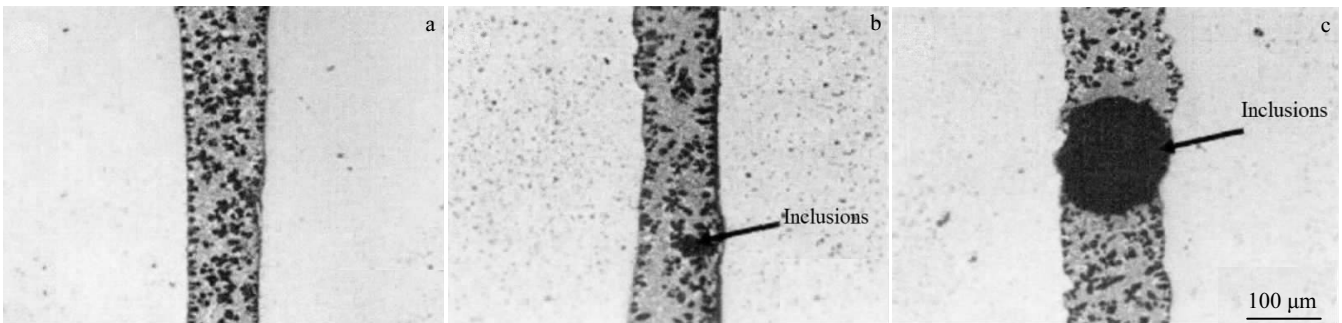


Fig.6 Microstructures of the brazed joints with different oxygen contents: (a) sample 1, (b) sample 4, and (c) sample 5

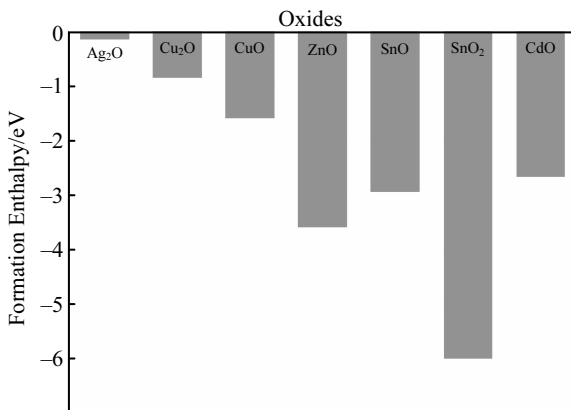


Fig.7 Formation enthalpy of various oxides in the FAg737 filler metal

that the filler metals are significantly deformed and some surface deformation bands are observed (Fig.10b). Because the deformation between the 316LN substrate and the filler metal cannot match, significant strain concentration occurs in the vicinity of the interface. Deformation in the strain concentration area is much higher than that in other areas, leading to the formation of microcracks. After 160 h of thermal cycling, the damage near the interface is further developed, with the formation of continuous cracks (Fig.10c). Due to friction between both sides of the interface after crack formation, the filler metal near the crack is squeezed out^[16,17].

Fig.11a shows that the defects in the brazing seam before the fatigue testing are solid-state inclusions without obvious cracks (Fig.11a). After 40 h of thermal cycling, these inclusions began to form microcracks (Fig.11b). The reason for the microcrack initiation is that these inclusions are brittle oxides which cannot undergo plastic deformation. Thus, the deforma-

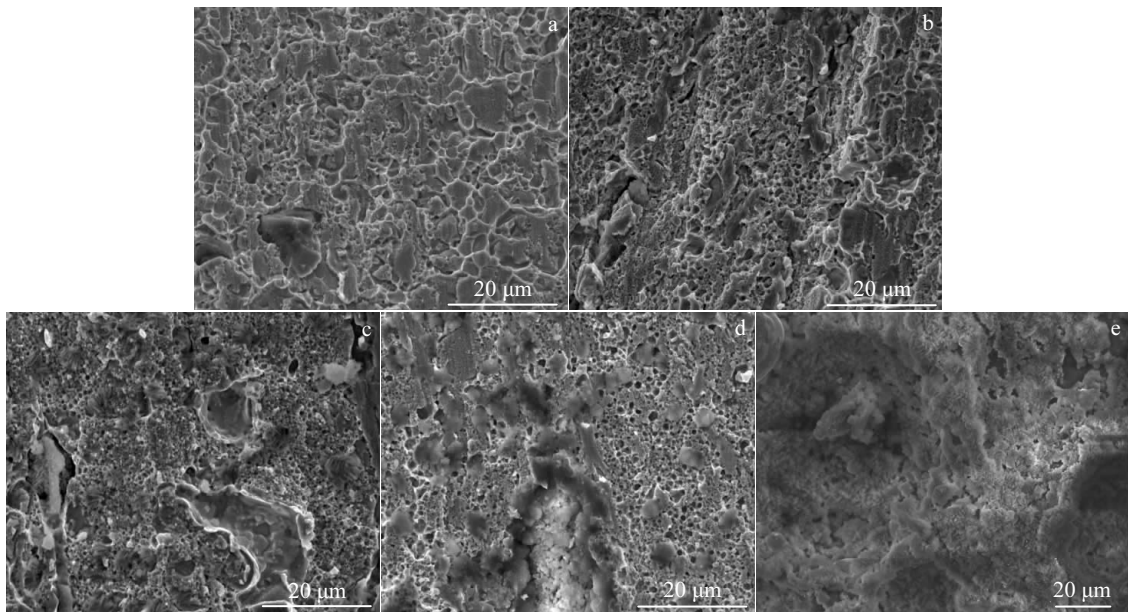


Fig.8 Fracture morphologies of brazed joints using filler metals with different oxygen contents: (a) sample 2, (b) sample 4, (c) sample 5, (d) sample 6, and (e) sample 8

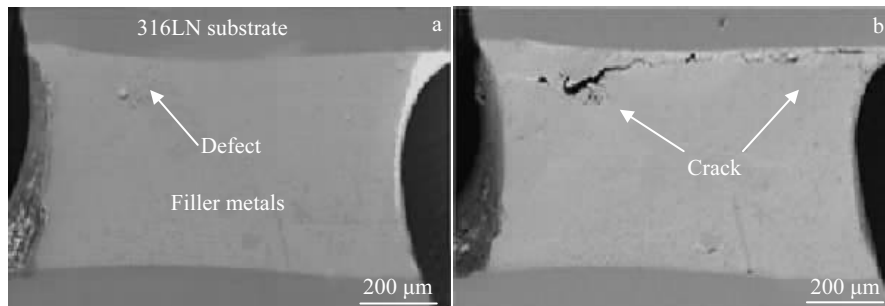


Fig.9 Macroscopic deformation morphologies of brazed joints: (a) before fatigue test and (b) after 100 h of thermal cycling

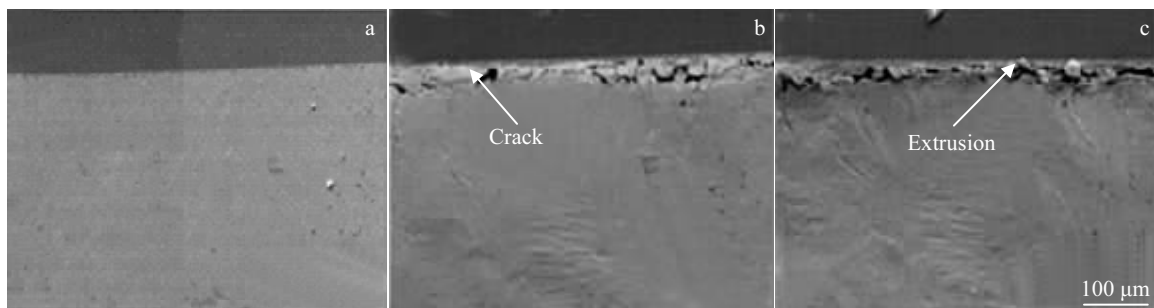


Fig.10 Micro-deformation morphologies of interfaces before fatigue testing (a), and after 100 h (b) and 160 h (c) of thermal cycling

tion between the inclusion and surrounding filler metal cannot match, leading to the formation of cracks. After the crack formation, more severe strain concentration occurs around the cracks, resulting in the rapid crack expansion. Subse-

quently, cracks are widened and extended to the interface (Fig.11c), resulting in the connection of these cracks. Finally, these cracks substantially reduce the brazed joint strength^[18].

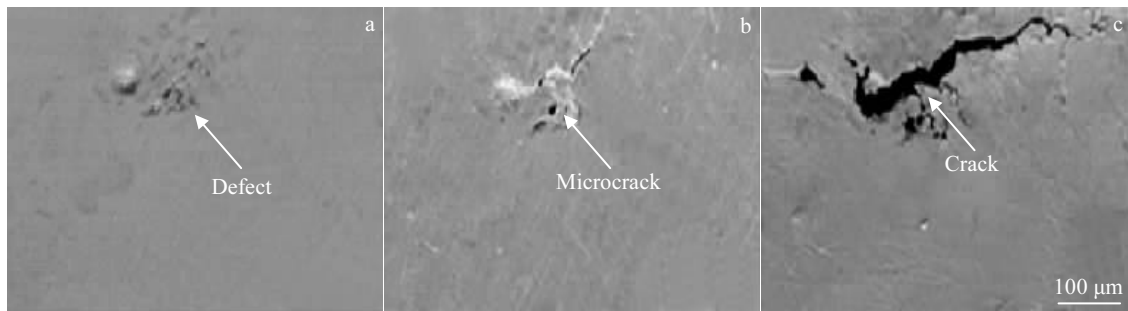


Fig.11 Morphologies before fatigue testing (a) and after 40 h (b) and 100 h (c) of thermal cycling

3 Conclusions

1) The apparent activation energy of the brazing filler metal increases continuously with increasing the oxygen content. The phase change activation energies of two alloys with oxygen contents of 26 and 2300 $\mu\text{g}\cdot\text{g}^{-1}$ are 46.554 and 77.564 kJ/mol, respectively. Thus, samples with higher oxygen content exhibit a longer melting time under the same conditions.

2) The tensile strength of the brazed joints decreases nonlinearly with increasing the oxygen content in the filler metal. In order to ensure a good performance of brazing filler metals, the filler metal oxygen content should be controlled less than 200 $\mu\text{g}\cdot\text{g}^{-1}$.

3) During the fatigue testing, the brazing defects are also found to be sources of fractures and cracking.

References

- Ding W F, Xu J H, Shen M et al. *Materials Science and Engineering A*[J], 2006, 430(1-2): 301
- Ganjeh E, Sarkhosh H, Khorsand H et al. *Materials & Design*[J], 2012, 39(311): 33
- Taranets N Y, Jones H. *Materials Science and Engineering A*[J], 2004, 379(1-2): 251
- Dai X, Cao J, Liu J et al. *Materials & Design*[J], 2015, 87: 53
- Sui F F, Long W M, Liu S X et al. *Materials & Design*[J], 2013, 46(4): 605
- Laik A, Mishra P, Bhanumurthy K et al. *Acta Materialia*[J], 2013, 61(1): 126
- Chen W X, Xue S B, Wang H et al. *Materials & Design*[J], 2010, 31(4): 2196
- Shiue R K, Wu S K, Chen S Y et al. *Acta Materialia*[J], 2003, 51(7): 1991
- Ji F, Xue S, Dai W et al. *Materials & Design*[J], 2012, 42: 156
- Xue P, Xue S B, Shen Y F et al. *Materials & Design*[J], 2014, 60(8): 1
- Webb E B, Hoyt J J. *Acta Materialia*[J], 2008, 56(8): 1802
- Yang J L, Xue S B, Xue P et al. *Materials & Design*[J], 2014, 64(9): 110
- Ye H, Xue S B, Luo J D et al. *Materials & Design*[J], 2013, 46(4): 816
- Zhang L X, Feng J C, He P et al. *Materials Science and Engineering A*[J], 2006, 200: 3713
- Long W M, Zhang G X, Zhang Q K et al. *Scripta Materialia*[J], 2015, 110(11): 41
- Dai W, Xue S B, Lou J Y et al. *Materials & Design*[J], 2012, 42: 395
- Eijk C V D, Sallom Z K, Akselsen O M et al. *Scripta Materialia*[J], 2008, 58(9): 779
- Li Y L, He P, Feng J C. *Scripta Materialia*[J], 2006, 55(2): 171

氧含量对银基粉状钎料熔化特性和钎焊接头性能的影响

龙飞¹, 张冠星², 何鹏^{1,2}, 耿慧远¹, 丁天然², 马佳²

(1. 哈尔滨工业大学 先进焊接与连接国家重点实验室, 黑龙江 哈尔滨 150006)

(2. 郑州机械研究所有限公司 新型钎焊材料与技术国家重点实验室, 河南 郑州 450001)

摘要: 通过第一性原理计算和试验等多种分析方法研究氧含量对熔化特性以及钎焊接头力学性能的影响。结果表明, 钎料的表现活化能随着钎料中氧含量的增加而增加, 导致了熔化时间增加。随着钎料中氧含量的增加, 钎焊接头的抗拉强度呈现非线性下降, 为了确保钎料的良好性能, 应该将钎料中的氧含量控制在 200 $\mu\text{g}\cdot\text{g}^{-1}$ 以下。根据疲劳试验结果, 氧元素引起的钎焊缺陷被认为是裂纹的源头, 该研究提供了氧含量对银基粉状钎料钎焊过程影响的详细机制。

关键词: 氧含量; 熔化特性; 力学性能

作者简介: 龙飞, 男, 1993年生, 硕士, 哈尔滨工业大学先进焊接与连接国家重点实验室, 黑龙江 哈尔滨 150006, E-mail: justlff@126.com